Author Manuscript

Author Manuscript

Author Manuscript

Author Manuscript

HHS Public Access

Author manuscript

J Surg Res. Author manuscript; available in PMC 2015 September 21.

Published in final edited form as:

J Surg Res. 2014 July ; 190(1): 111–118. doi:10.1016/j.jss.2014.02.021.

Targeting of BRAF resistant melanoma via extracellular matrix metalloproteinase inducer receptor

Matthew R Zeiderman, BA[1], **Michael E Egger, MD MPH**[1], **Charles W Kimbrough, MD**[1], **Christopher G England, MS**[2], **Tess V Dupre, BS**[2], **Kelly M McMasters, MD PhD**[1], and **Lacey R McNally, PhD**[3]

[1] Hiram C. Polk Jr. MD Department of Surgery, University of Louisville, Louisville, Kentucky

[2] Department of Pharmacology & Toxicology, University of Louisville, Louisville, Kentucky

[3] Department of Medicine, University of Louisville, Louisville, Kentucky

Abstract

The BRAF inhibitor Vemurafenib (PLX) has shown promise in treating metastatic melanoma, but most patients develop resistance to treatment after 6 months. We identified a transmembrane protein, extracellular matrix metalloproteinase inducer (EMMPRIN) as a cell surface receptor highly expressed by PLX-resistant melanoma. Using an S100A9 ligand, we created an EMMPRIN targeted probe and liposome that binds to melanoma cells *in vivo*, thus designing a novel drug-delivery vehicle.

Methods—PLX-resistant cells were established through continuous treatment with PLX-4032 over the course of 1 year. Both PLX-resistant and sensitive melanoma cell lines were evaluated for expression of unique cell-surface proteins which identified EMMPRIN as an overexpressed protein in PLX0-resistant cellsS100A9 is a ligand for EMMPRIN. To design a probe for EMMPRIN, S100A9 ligand was conjugated to a CF-750 NIR-dye. EMMPRIN targeted liposomes were created to encapsulate CF-750 NIR-dye. Liposomes were characterized by SEM, flow-cytometry, and *in vivo* analysis. A2058PLX and A2058 cells were subcutaneously injected into athymic mice. S100A9 liposomes were IV injected and tumor accumulation was evaluated using NIR-fluorescent imaging.

Results—Western blot and flow cytometry demonstrated that PLX-sensitive and resistant A2058 and A375 melanoma cells highly express EMMPRIN. S100A9 liposomes were measured to be 200nm diameter and uniformly sized. Flow cytometry demonstrated 100X more intracellular dye uptake by A2058 cells treated with S100A9 liposomes compared to untargeted liposomes. *In vivo* accumulation of S100A9 liposomes within subcutaneous A2058 and A2058PLX tumors was observed from 6 to 48 hours, with A2058PLX accumulating significantly higher levels (p=0.001626).

Correspondence should be directed to Lacey McNally: lrmcna01@louisville.edu, University of Louisville, Department of Medicine, 505 S Hancock, CTR building Rm 307, Louisville, KY 40202, Phone:502-852-2288, Fax number:502-852-2123.

M. Zeiderman contributed to experiments for Fig. 1, 2, 3 as well as primary author of manuscript. M. Egger contributed to concept design and Fig. 1. C Kimbrough assisted with Figs 2-3. C. England assisted with experiments for Fig. 2 and liposome preparation. T. Dupre assisted with data collection for Fig. 2. K. McMasters contributed to Fig. 3 as well as manuscript editing and preparation as well as project funding. L. McNally contributed to concept design, editing and preparation of the manuscript, experimental design, and project funding. This project was supported by grant R25-CA-134283 from the National Cancer Institute.

Author Manuscript Author Manuscript Author Manuscript Author Manuscript

Conclusion—EMMPRIN-targeted liposomes via an S100A9 ligand are a novel, targeted delivery system which could provide improved EMMPRIN specific drug delivery to a tumor.

Keywords

melanoma; BRAF; EMMPRIN; liposome; S100A9; nanoparticles; near-infrared; resistant; imaging; targeted drug delivery

1 Introduction

It is estimated that almost 77,000 Americans will develop melanoma in 2013, and almost 9,500 will die of the disease (1). A localized tumor is easily resected if detected early, but approximately 5% of patients will develop metastatic spread for which surgical intervention may be limited (2). Of those with metastatic disease, only 5 to 10% achieve a complete response to chemotherapeutic intervention (2, 3). Combination chemotherapy has been attempted, but this has not proven to significantly improve survival of patients with metastatic disease (4-6). Furthermore, traditional chemotherapeutic methods often result in significant systemic cytotoxicity, and consequently cannot always be given at therapeutically useful doses (4, 5, 7-9). Cancer-cell targeted nanoparticles provide a novel mechanism to overcome this obstacle and provide cell-specific drug delivery and tumor imaging while reducing systemic toxicity (7, 10-12).

A newly emerging concept for the diagnosis, treatment, and *in situ* imaging and monitoring of metastatic melanoma is the use theranostic nanoparticles. Theranostic agents can be simultaneously designed as both drug-delivery and imaging vehicles via the incorporation of fluorescent dye imaging agents and chemotherapeutic drugs (13-15). Importantly, peptides can be conjugated to the nanoparticles to target cancer cells.The nanoparticles can then be injected either locally or systemically and imaged in real-time using non-invasive methods such as MRI, CT, or PET (13, 15). In particular, using near-infrared (NIR) fluorescent particles allows for particularly sensitive *in* vivo imaging of tumor location and progression, as the narrow emission spectra of NIR fluorescent dyes (700-900 nm) have the advantages of reduced autofluorescence, reduced tissue scattering, and greater depth of penetration (13, 15, 16).

We sought to identify a novel tumor-cell specific drug-delivery and imaging vector for the treatment of metastatic melanoma. Clearly, not all tumor cell surface proteins are equally ideal drug targets, with some expressed at higher levels than others. Extracellular matrix metalloproteinase inducer (EMMPRIN), or CD147, is an integral trans-membrane protein that is highly expressed in metastatic melanoma and other malignant cells and plays a role in the angiogenesis, progression and metastasis of the disease (17-22). Furthermore, EMMPRIN is expressed at very low levels in somatic cells, thus making it an ideal cancer cell specific target (17,18, 21). EMMPRIN dimerizes with the calcium binding protein S100A9 (18). Using an S100A9 ligand and NIR-fluorescent dye, we have created an EMMPRIN targeted liposome and fluorescent probe that selectively binds melanoma cells *in vitro* and *in vivo*, thus designing a novel vehicle for *in vivo* drug delivery and imaging to provide greater efficacy of cancer treatment while reducing systemic toxicity.

Author Manuscript Author Manuscript Author Manuscript Author Manuscript

2. Methods

2.1 Cell Culture

Human melanoma cell lines A2058 and A375 were obtained from American Type Culture Collection (Rockville, MD). A2058, A2058PLX, A375, A375PLX, and MCF-7 (negative control) cell lines were cultured in cultured in Dulbecco's modified Eagle medium. ES-2 (clear cell ovarian carcinoma),MiaPaCa2 (pancreatic adenocarcinoma), and UM-SCC1 (head and neck squamous cell carcinoma) cell lines were cultured in RPMI as positive controls for EMMPRIN. All media were supplemented with 10% fetal bovine serum (Atlanta Biologicals, Lawrenceville, GA) and 1% Penicillin-Streptomycin. Cell culture reagents were purchased from Gibco (Life Technologies, Grand Island, NY). Cells were cultured at 37° C, 5% CO_2. Vemurafenib resistant cell lines, denoted A2058PLX and A375PLX, were grown under the same media and environmental conditions with the additional treatment of 10μM and 1.0μM Vemurafenib (PLX-4032) (Selleck Chemicals, Houston, TX) respectively, at each passage for one year to maintain resistance. Maintenance of Vemurafenib resistance was evaluated monthly via cell viability assay. Cell viability was determined at 24 h following treatment with Vemurafenib using the ATPlite assay system and read on the Advanced Molecular Imager 1000X (AMI) (Spectral Imaging Instruments, Tucson, AZ)(PerkinElmer, Waltham, MA). Percent cell viability was determined by dividing the treated cells' luminescence counts by the corresponding control cells.

2.2 Protein Analysis

A2058, A2058PLX, A375, A375PLX, MiaPaCa2, ES-2, UM-SCC1, and MCF-7 cells were plated in 6-well plates at 5×10^5 cells/well and allowed to attach for 24 h at 37° C, 5% CO_2. Whole cell protein lysates were collected using sodium orthovanadate (Sigma-Aldrich, St. Louis, MO) NuPAGE 4-12% Bis Tris gels were used for protein electrophoresis (Life Technologies, Grand Island, NY). Transfer to nitrocellulose membranes was performed using the iBLOT gel transfer device from Invitrogen (Life Technologies, Grand Island, NY). Odyssey blocking buffer was used for western blotting (LI-COR, Lincoln, NE). Primary antibodies for western blot were incubated at 4°C overnight at the following concentrations: actin (1:2000) (Pierce Chemicals, Thermo Fisher Scientific, Rockford, IL) and EMMPRIN/CD147 (1:500) (Abcam Biochemicals, Cambridge, England). Blots were given 3X for ten minutes per wash prior to incubation in secondary antibodies. Secondary antibodies were rabbit and mouse IR-Dye antibodies (LI-COR, Lincoln, NE). The secondary antibodies were incubated for 1 h at 25°C (1:3000) in Odyssey blocking buffer and washed again 3X for 10 minutes per wash prior to development. Blots were developed and analyzed using the Odyssey Infrared Imaging System (LI-COR, Lincoln, NE). Relative abundance of EMMPRIN was determined based on B-actin using dosimetry.

2.3 Liposome and probe design

To design a probe for EMMPRIN expressing cells, S100A9 ligand (Prospec, Ness-Ziona, Israel) was conjugated to a CF-750-succinimidyl ester NIR-dye (Biotium, Hayward, CA). EMMPRIN targeted stealth liposomes were created to encapsulate CF-750 NIR-dye.

Author Manuscript Author Manuscript Author Manuscript Author Manuscript

All lipids will be purchased from Avanti Polar Lipids Inc., (Alabaster, AL). Once the bio-conjugated lipid was synthesized, the three structural lipids of the liposome were dissolved in an organic solvent (chloroform) and mixed together at 20 mg/mL (23).

After thoroughly mixing the lipids, organic solvent was evaporated using a rotary evaporator (Heidolph, Germany) to yield a thin film of lipid. The thin layer of lipid was rehydrated using distilled water and sonicated for the production of large, multilamellar vesicles encapsulating the necessary entities (CF 750 NIR-dye Biotium) at controlled temperatures dependent upon lipid combination within the liposomes and the targeting lipid (S100A9 ligand). Accurate sizing of the vesicles was controlled through sonication and filtering methods (extrusion method) to ensure particles were within the size limitations needed for *in vitro* applications (24).

Control liposomes contain a mixture of PEGylated lipid, egg phosphatidyl choline (PC), and 1,2-Dioleoyl-sn-Glycero-3-Phosphoethanolamine (DOPE) (3:4:1).

S100A9 liposomes contain mixture of egg phosphatidyl choline, nickel-chelating lipid DGS–NTA–Ni (1,2-dioleoyl-*sn*-glycero-3-{[*N*(5-amino-1-carboxypentyl)iminodiacetic acid]succinyl}(nickel salt)), and DOPE (4:2:1) to formulate proteoliposomes with proteins attached by metallochelation, including histidine (His)-tagged recombinant S100A9 protein (S100A9 6-Histidine).

2.4 Characterization of liposomes

Liposomes were verified using Scanning Electron Microscopy (SEM) (Phillips), UV-Visible Spectcopy (Cary UV-VIS spectrophotometer (Agilent, Santa Clara, CA) from 200nm to 900nm, and flow cytometry (25, 26).

2.5 Flow Cytometry

Both PLX-sensitive and resistant A2058 and A375 cell lines were evaluated utilizing flow cytometry for targeted-probe and/or -liposome uptake in comparison to untreated cells and non-targeted liposome. Histograms and scatter plots were used to illustrate the binding of probes and liposomes. MCF-7 breast cancer cells served as negative controls. ES-2 clear-cell ovarian carcinoma and S2VP10 pancreatic carcinoma cell lines served as positive controls. All cell lines were plated in 6-well plates at 5×10^5 cells/well and allowed to attach for 24 h at 37° C, 5% CO_2. Cells were scraped and incubated for 2 h as naked liposome, CF-750 dye alone, S100A9 probe (S100A9 ligand conjugated to CF-750), or S100A9 liposome encapsulating CF-750 dye. Flow cytometry was performed using the BD FACS Canto flow cytometer (BD Biosciences, San Jose, CA) with 50,000 events and cell counts analyzed with FlowJo software (TreeStar, Inc., Ashland, OR).

2.6 In Vivo Analysis

In vivo studies were performed under IACUC approval. Mice were allowed one week for acclimation prior to tumor injection. 5 female 6-week old athymic mice (Harlan Laboratories) each received subcutaneous tumors of 5×10^6 cells with either the A2058 or A2058PLX cell line. Two weeks after tumor injection S100A9 probe and S100A9 liposome

Author Manuscript Author Manuscript Author Manuscript Author Manuscript

were IV injected through the tail vein at 5 O.D. in separate experiments. Isoflurane anesthesia, 2.0%, was administered and maintained during IV tail vein injection and imaging. Tumor accumulation of CF-750 NIR dye was evaluated by the region of interest method every 6 h for 48 h. Near IR (NIR) was evaluated using the AMI 1000X (Spectral Imaging Instruments, Tucson, AZ) using a 675 excitation filter and a 750 emission filter.

3 Results

3.1 Human melanoma cell lines express EMMPRIN

Using two human melanoma cells lines, we identified EMMPRIN as a novel cell-surface receptor highly expressed by both wild-type and Vemurafenib-resistant (denoted PLX) melanoma cells (Fig 1-A-B). Western blot analysis demonstrates that EMMPRIN is expressed in A2058, A2058PLX, A375, and A375PLX cell lines.EMMPRIN is differentially expressed by the Vemurafenib-resistant A2058 and A375 human melanoma cell lines and the PLX resistant cells have twice the EMMPRIN expression as the Vemurafenib-sensitive melanoma counterparts (Fig 1B). This finding is particularly important in the selection of an extracellular cancer-cell specific target for tumor imaging and drug delivery for patients with metastatic disease that is resistant to front-line Vemurafenib treatment. S2VP10 is a pancreatic cancer cell line and ES-2 is a clear-cell ovarian cancer cell line that highly express EMMPRIN and served as the positive controls. MCF7 breast cancer cells do not express EMMPRIN and served as a negative control.

3.2 Characterization of S100A9 probe and liposome *in vitro*

Based on the finding that S100A9 is a ligand for EMMPRIN, we designed both an S100A9 ligand conjugated to a CF-750 Near-Infrared (NIR) dye (S100A9 probe) and a liposome conjugated to S100A9 ligand and encapsulating CF-750 NIR-dye (S100A9 liposome) (Fig. 2). Absorption spectra of the near-infrared CF-750 dye were as expected and remained unchanged by encapsulation of liposome or when conjugated to S100A9 ligand to make the S100A9 probe (Fig. 2A). Scanning electron microscopy (SEM) demonstrated that liposomes are 200nm (+/− 30 and appear to be uniform in shape (Fig. 2B). Flow cytometry was performed to analyze *in vitro* binding of S100A9 probe and S100A9 liposome to A2058 human melanoma cells. An untargeted liposome encapsulating CF-750 NIR dye and an untreated cell population incubated with dye alone were the control conditions. Flow cytometry demonstrated that two separate batches of S100A9 probe effectively bound to A2058 cells, although there was non-specific binding to the cells which we attribute to the reactive group on the CF-750 dye non-selectively binding to cell-surface receptors (Fig. 2C). Importantly, both batches of S100A9 probe bound to A2058 cells ten-fold more effectively than the untargeted die alone. S100A9 liposome bound to EMMPRIN expressing A2058 cells more than 100X more efficiently than the untargeted liposome (Fig. 2D). These results confirm that multiple human melanoma cell lines express EMMPRIN and that S100A9 ligand selectively binds EMMPRIN expressing cells *in vitro.* Flow cytometry demonstrated that binding of S100A9 liposome to cells, as demonstrated by CF-750 NIR-dye delivery, directly corresponds with the level of EMMPRIN expression observed in western blot (Fig S1). The binding of S100A9 probe demonstrates a similar trend. S100A9 liposome effectively bound to A2058 (28.8%) and A2058PLX (33.3%) human melanoma cells. As

Author Manuscript Author Manuscript Author Manuscript Author Manuscript

expected, S100A9 liposome demonstrated more efficient binding to A375 (43.5%) and A375PLX (47.5%) cells which express higher levels of EMMPRIN than A2058 strains (Fig S1). ES-2 cells served as a positive control and demonstrated high binding by S100A9 probe (48%) and liposome (65.2%). S2VP10 cells served as a second positive control and also demonstrated high binding to S100A9 probe (45.1%) and S100A9 liposome (40.0%) (Fig S1). MCF-7 cells served as a negative control and exhibited much less efficient binding to S100A9 probe (5.0%) and liposome (20.2%) than cell lines which express high EMMPRIN (Fig S1).

3.3 *In vivo* binding of S100A9 liposome and S100A9 probe

Our main aim was to obtain specific uptake of liposomes by both PLX resistant and sensitive tumors via a systemic injection. S100A9 probe and S100A9 liposome both effectively bound A2058 and A2058PLX subcutaneous melanoma tumors. S100A9 probe was injected as a preliminary study and demonstrated equal efficacy with tumor accumulation observed from 6 to 48 hours. One hour after injection, the S100a9 liposomes levels were $2.62E^5$ (A2058) and $2.29E^5$(A2058PLX) (Fig 3B). The liposomes continued to accumulate and by 48h were at $3.5E^6$ (A2058) and $1.05E^7$ (A2058PLX). Significant differences were observed in accumulation of the S100a9 liposome in A2058PLX tumors in comparison to A2058 p=0.001626 (Fig 3B).

4. Discussion

The main aim of this study was to identify a cell-surface receptor highly expressed by both Vemurafenib sensitive and resistant melanoma cell. Our results serve as a proof of principle that EMMPRIN expression provides a novel target for cell-specific targeting of metastatic melanoma. Furthermore, we show that S100A9 ligand can be used to efficiently target liposomes to metastatic melanoma cells for cancer-cell specific drug-delivery and theranostic imaging *in vivo*.

It is well documented that engineered liposomes and nanoparticles have the ability to deliver larger doses of drugs while preventing systemic cytotoxicity *in vivo* via receptor-mediated endocytosis drug delivery (7, 11, 17, 27, 28). Notable examples of untargeted liposomal drug delivery to tumors include Doxil, a liposomal preparation encapsulating Doxorubicin for the treatment of multiple types of cancer, and a newly designed silica nanoparticle conjugated to folic acid and loaded with Doxorubicin (11, 29). While untargeted therapy has shown potential, it is still less efficient than receptor-targeted drug delivery. Patients may be exposed to unintentional systemic toxicity if the drug were to diffuse out of the liposome or if there is liposomal clearance and degradation by systemic macrophages. To increase treatment efficacy, peptides have been conjugated to liposomes to provide cancer cell targeted drug delivery, and such methods have been used in the treatment of breast cancer, refractory ovarian cancer, Kaposi’s sarcoma, and melanoma (10, 12, 30-32). Our findings are unique in the identification of a cell-surface receptor that is expressed in multiple human melanoma cell lines, EMMPRIN, as well as a ligand that specifically binds EMMPRIN in Vemurafenib resistant cells. Furthermore, use of a CF-750 NIR-dye provided a method

Author Manuscript Author Manuscript Author Manuscript Author Manuscript

allowing for *in vivo* fluorescent imaging, thus enabling not only cell-specific drug delivery, but also efficient, non-invasive monitoring of tumor progression.

The potential clinical utility of S100A9 liposomes for targeting BRAF resistant melanoma cells was observed via flow cytometry and *in vivo* subcutaneous tumors. Relative EMMPRIN expression was lowest in A2058 cells in comparison to A2058PLX, A375, and A375PLX cell lines. Because A2058 and A2058PLX cells also demonstrated lower EMMPRIN expression, less efficient *in vitro* binding to S100A9 probe and liposome, and exhibit more aggressive and rapid growth in culture than the A375 strains, we chose to evaluate these cells to more closely approximate clinical presentation. S100A9 ligand and liposome efficiently bound A2058 and A2058PLX cells both *in vitro* and *in vivo.* These findings enhance the clinical utility of EMMPRIN targeted liposomes, as our results demonstrate that even melanoma strains such as A2058 which express lower levels of EMMPRIN than other tumors can be targeted without undesired accumulation in non-target tissue. While flow cytometry demonstrated non-specific binding of CF-750 dye to A2058 cells, we believe this to be a result of reactive groups on the free-floating dye reacting with extracellular proteins on the cells and not a result of the dye targeting the cells. *In vivo*, there did not appear to be any non-specific binding, as both probe and liposome accumulated only in the tumors. Furthermore, the flow cytometry results demonstrated more than a 100-fold increase in binding and dye uptake by A2058 melanoma cells with S100A9 liposomes compared to the untargeted-liposomes. This suggests that dye uptake occurs via receptor-mediated endocytosis, not unselective dye binding.

Many groups have designed cancer-receptor targeted nanoparticles. For instance, Her2 targeted iron-oxide nanoparticles have been designed for imaging and cell-targeted drug delivery in ovarian cancer (12). Two different groups have attempted cell-specific targeting of melanoma cells *in vivo*, demonstrating methods that could potentially reduce systemic toxicity in chemotherapeutic drug delivery. Alpha-melanocyte stimulating hormone has been conjugated to human ferritin nanoparticles; this approach demonstrated *in vivo* melanoma tumor-accumulation at 24 hours (31). Another group used EP1, a monoclonal antibody to the human melanoma-specific antigen CSPG4, conjugated to a single ferritin cage and encapsulating cisplatin (32). While the *in vivo* results of other groups are notable, a significant clinical disadvantage of tumor-targeting via metal nanoparticles is accumulation in non-target organs, such as the liver and spleen (33, 34). As chemotherapy requires multiple doses over weeks or months, metal toxicity due off-target organ accumulation poses a major clinical hurdle for metal nanoparticles, particularly those containing iron. Lipid based liposomes overcome this issue. Neither S100A9 liposome nor probe accumulated in untargeted tissues other than the bladder, which is to be expected as liposomes are renally cleared. These findings indicate that S100A9 liposomes are not rapidly cleared from the circulation by systemic macrophages of the reticuloendothelial system. Instead, the liposomes continually circulate through the blood and either specifically bind to tumors or are eliminated through the urine. By continually circulating in this manner, S100A9 liposomes may allow for more prolonged and sustained drug delivery and offer advantages over metal nanoparticles targeted to cancer cells. Additionally, the lipid

Author Manuscript Author Manuscript Author Manuscript Author Manuscript

composition of liposomes is non-toxic, thus circumventing the clinical obstacle of non-target organ toxicity and metal poisoning posed by metal nanoparticles.

Furthermore, while the skin is a highly vascular tissue, it receives blood from small arterioles and capillary beds. S100A9 liposomes are approximately 200nm in diameter and therefore small enough to navigate capillaries and reach tumors in any vascularized tissue without becoming stuck in 3 μm diameter capillaries (35). Metastatic melanoma tumors are more likely to be found in organs which have a greater vascular supply than skin, such as the liver and lungs. The ability of S100A9 liposomes to navigate small vessels is encouraging and it is likely that accumulation of S100A9 liposomes would be even greater in tumors located within highly vascularized tissue with larger blood vessels.

EMMPRIN targeting with S100A9 liposomes may have applications for the treatment and imaging of other cancers as well. EMMPRIN has been shown to be highly expressed in squamous cell carcinoma of the head and neck, glioblastoma multiforme, pancreatic and hepatocellular carcinomas, medullary breast adenocarcinoma, and chromophobe renal cell carcinoma (21, 36). Our western blot and flow cytometry results with ES-2 clear-cell ovarian carcinoma and S2VP10 pancreatic carcinoma cell lines, which express high EMMPRIN and efficiently bind S100A9 probe and S100A9 liposome, demonstrate the potential applicability of EMMPRIN targeting for treatment of malignancies other than melanoma. Using an S100A9 liposome, clinicians and scientists may be able to develop therapies for other EMMPRIN expressing neoplasms that resist chemotherapeutic treatment, cancers that are difficult to target with current drugs and treatment regimens, or enhance the efficacy drugs that accumulate in off-target organs. For physicians trying to treat resistant or recurrent melanoma, the ability to deliver combination therapy is crucial. While agents like Vemurafenib have shown initial promise, most patients develop resistance to the drug. Vemurafenib inhibits BRAF, a proto-oncogenic kinase high in the Map kinase/ERK signaling pathway. Despite its importance in driving cancer cell growth, a BRAF mutation alone does not result in malignancy, as BRAF is mutated in benign nevi (37). Cells harboring a BRAF mutation certainly have acquired other mutations, including up-regulation of additional growth pathways or survival mechanisms such as expression of the multi-drug resistance proteins MRP 1-3 and the multidrug resistant efflux pump MDR-1. These mechanisms prevent intracellular accumulation of drugs and confer resistance to other chemotherapeutics in addition to Vemurafenib (38, 39). Thus, a way to concentrate drug delivery is essential. Receptor-mediated endocytosis and drug delivery via S100A9 liposomes may help to deliver therapeutic drug concentrations to these difficult to treat tumors and increase treatment efficacy if drugs can be successfully encapsulated and delivered in S100A9 liposomes.

5 Conclusions

This study demonstrates that EMMPRIN/CD147 is a suitable target for cancer cell targeted drug delivery and *in vivo* tumor imaging using an S100A9 ligand conjugated to a liposome. Our findings could potentially be used for as a targeted delivery system for the future treatment of melanoma and other EMMPRIN expressing neoplasms. To further test S100A9 liposomes, studies will need to demonstrate successful encapsulation of drugs inside of the

Author Manuscript Author Manuscript Author Manuscript Author Manuscript

liposomes and efficacious *in vivo* drug delivery. At present, a metastatic melanoma mouse-model has not been achieved, as past attempts have led to diffuse, systemic seeding of cells instead of creation of a localized tumor. The creation of such a living model of melanoma will enable further validation of S100A9 liposomes for *in vivo* tumor imaging and drug delivery. Furthermore, chemotherapeutic agents must be identified that can be packaged within the liposomes for cancer-cell targeted drug delivery.

Supplementary Material

Refer to Web version on PubMed Central for supplementary material.

Acknowledgements

This project was supported by grant R25-CA-134283 from the National Cancer Institute. This project was also supported by the James Graham Brown Cancer Center at the University of Louisville.

References

1. Society, AC. Cancer Facts and Figures 2013. American Cancer Society; Atlanta: 2013.
2. Ravnan MC, Matalka MS. Vemurafenib in patients with BRAF V600E mutation-positive advanced melanoma. Clin Ther. 2012; 34:1474–1486. [PubMed: 22742884]
3. Serrone L, Zeuli M, Sega FM, Cognetti F. Dacarbazine-based chemotherapy for metastatic melanoma: thirty-year experience overview. J Exp Clin Cancer Res. 2000; 19:21–34. [PubMed: 10840932]
4. Atkins MB, Hsu J, Lee S, Cohen GI, Flaherty LE, et al. Phase III trial comparing concurrent biochemotherapy with cisplatin, vinblastine, dacarbazine, interleukin-2, and interferon alfa-2b with cisplatin, vinblastine, and dacarbazine alone in patients with metastatic malignant melanoma (E3695): a trial coordinated by the Eastern Cooperative Oncology Group. Journal of clinical oncology : official journal of the American Society of Clinical Oncology. 2008; 26:5748–5754. [PubMed: 19001327]
5. Algazi AP, Weber JS, Andrews SC, Urbas P, Munster PN, et al. Phase I clinical trial of the Src inhibitor dasatinib with dacarbazine in metastatic melanoma. British journal of cancer. 2012; 106:85–91. [PubMed: 22127285]
6. Jiang G, Li RH, Sun C, Jia HY, Lei TC, et al. Efficacy and safety between temozolomide alone and temozolomide-based double therapy for malignant melanoma: a meta-analysis. Tumour biology : the journal of the International Society for Oncodevelopmental Biology and Medicine. 2013
7. Chen S, Zhao X, Chen J, Chen J, Kuznetsova L, et al. Mechanism-based tumor-targeting drug delivery system. Validation of efficient vitamin receptor-mediated endocytosis and drug release. Bioconjugate chemistry. 2010; 21:979–987. [PubMed: 20429547]
8. Allen TM. Ligand-targeted therapeutics in anticancer therapy. Nature reviews. Cancer. 2002; 2:750–763. [PubMed: 12360278]
9. Finn L, Markovic SN, Joseph RW. Therapy for metastatic melanoma: the past, present, and future. BMC medicine. 2012; 10:23. [PubMed: 22385436]
10. Ferrari M. Cancer nanotechnology: opportunities and challenges. Nature reviews. Cancer. 2005; 5:161–171. [PubMed: 15738981]
11. Luo Z, Ding X, Hu Y, Wu S, Xiang Y, et al. Engineering a Hollow Nanocontainer Platform with Multifunctional Molecular Machines for Tumor-Targeted Therapy in Vitro and in Vivo. ACS nano. 2013
12. Satpathy M, Wang L, Zielinski R, Qian W, Lipowska M, et al. Active Targeting Using HER-2-Affibody-Conjugated Nanoparticles Enabled Sensitive and Specific Imaging of Orthotopic HER-2 Positive Ovarian Tumors. Small (Weinheim an der Bergstrasse, Germany). 2013

Author Manuscript Author Manuscript Author Manuscript Author Manuscript

13. Ryu JH, Koo H, Sun IC, Yuk SH, Choi K, et al. Tumor-targeting multi-functional nanoparticles for theragnosis: new paradigm for cancer therapy. Adv Drug Deliv Rev. 2012; 64:1447–1458. [PubMed: 22772034]
14. Parveen S, Misra R, Sahoo SK. Nanoparticles: a boon to drug delivery, therapeutics, diagnostics and imaging. Nanomedicine : nanotechnology, biology, and medicine. 2012; 8:147–166.
15. Ahmed N, Fessi H, Elaissari A. Theranostic applications of nanoparticles in cancer. Drug discovery today. 2012; 17:928–934. [PubMed: 22484464]
16. Janib SM, Moses AS, MacKay JA. Imaging and drug delivery using theranostic nanoparticles. Advanced Drug Delivery Reviews. 2010; 62:1052–1063. [PubMed: 20709124]
17. Nishibaba R, Higashi Y, Su J, Furukawa T, Kawai K, et al. CD147-targeting siRNA inhibits cell-matrix adhesion of human malignant melanoma cells by phosphorylating focal adhesion kinase. The Journal of dermatology. 2012; 39:63–67. [PubMed: 21967109]
18. Hibino T, Sakaguchi M, Miyamoto S, Yamamoto M, Motoyama A, et al. S100A9 is a novel ligand of EMMPRIN that promotes melanoma metastasis. Cancer research. 2013; 73:172–183. [PubMed: 23135911]
19. Kanekura T. Chen X CD147/basigin promotes progression of malignant melanoma and other cancers. Journal of dermatological science. 2010; 57:149–154. [PubMed: 20060267]
20. Kanekura T, Chen X, Kanzaki T. Basigin (CD147) is expressed on melanoma cells and induces tumor cell invasion by stimulating production of matrix metalloproteinases by fibroblasts. International journal of cancer. Journal international du cancer. 2002; 99:520–528. [PubMed: 11992541]
21. Riethdorf S, Reimers N, Assmann V, Kornfeld JW, Terracciano L, et al. High incidence of EMMPRIN expression in human tumors. International journal of cancer. Journal international du cancer. 2006; 119:1800–1810. [PubMed: 16721788]
22. Tang Y, Nakada MT, Kesavan P, McCabe F, Millar H, et al. Extracellular matrix metalloproteinase inducer stimulates tumor angiogenesis by elevating vascular endothelial cell growth factor and matrix metalloproteinases. Cancer research. 2005; 65:3193–3199. [PubMed: 15833850]
23. Immordino ML, Dosio F, Cattel L. Stealth liposomes: review of the basic science, rationale, and clinical applications, existing and potential. International journal of nanomedicine. 2006; 1:297–315. [PubMed: 17717971]
24. Kang MJ, Park SH, Kang MH, Park MJ, Choi YW. Folic acid-tethered Pep-1 peptide-conjugated liposomal nanocarrier for enhanced intracellular drug delivery to cancer cells: conformational characterization and in vitro cellular uptake evaluation. International journal of nanomedicine. 2013; 8:1155–1165. [PubMed: 23515421]
25. Bibi S, Kaur R, Henriksen-Lacey M, McNeil SE, Wilkhu J, et al. Microscopy imaging of liposomes: from coverslips to environmental SEM. International journal of pharmaceutics. 2011; 417:138–150. [PubMed: 21182914]
26. Adler K, Schiemann J. Characterization of liposomes by scanning electron microscopy and the freeze-fracture technique. Micron and Microscopica Acta. 1985; 16:109–113.
27. Xiong MP, Yanez JA, Remsberg CM, Ohgami Y, Kwon GS, et al. Formulation of a geldanamycin prodrug in mPEG-b-PCL micelles greatly enhances tolerability and pharmacokinetics in rats. Journal of controlled release : official journal of the Controlled Release Society. 2008; 129:33–40. [PubMed: 18456363]
28. Allen TM, Cullis PR. Liposomal drug delivery systems: From concept to clinical applications. Advanced Drug Delivery Reviews. 2013; 65:36–48. [PubMed: 23036225]
29. Barenholz Y. Doxil(R)--the first FDA-approved nano-drug: lessons learned. Journal of controlled release : official journal of the Controlled Release Society. 2012; 160:117–134. [PubMed: 22484195]
30. Lu RM, Chen MS, Chang DK, Chiu CY, Lin WC, et al. Targeted drug delivery systems mediated by a novel Peptide in breast cancer therapy and imaging. PLoS One. 2013; 8:e66128. [PubMed: 23776619]
31. Vannucci L, Falvo E, Fornara M, Di Micco P, Benada O, et al. Selective targeting of melanoma by PEG-masked protein-based multifunctional nanoparticles. International journal of nanomedicine. 2012; 7:1489–1509. [PubMed: 22619508]

Author Manuscript Author Manuscript Author Manuscript Author Manuscript

32. Falvo E, Tremante E, Fraioli R, Leonetti C, Zamparelli C, et al. Antibody-drug conjugates: targeting melanoma with cisplatin encapsulated in protein-cage nanoparticles based on human ferritin. Nanoscale. 2013

33. Khlebtsov N, Dykman L. Biodistribution and toxicity of engineered gold nanoparticles: a review of in vitro and in vivo studies. Chemical Society Reviews. 2011; 40:1647–1671. [PubMed: 21082078]

34. Johnston HJ, Hutchison G, Christensen FM, Peters S, Hankin S, et al. A review of the in vivo and in vitro toxicity of silver and gold particulates: particle attributes and biological mechanisms responsible for the observed toxicity. Critical reviews in toxicology. 2010; 40:328–346. [PubMed: 20128631]

35. Wiedeman MP. Dimensions of blood vessels from distributing artery to collecting vein. Circulation research. 1963; 12:375–378. [PubMed: 14000509]

36. Dean NR, Newman JR, Helman EE, Zhang W, Safavy S, et al. Anti-EMMPRIN monoclonal antibody as a novel agent for therapy of head and neck cancer. Clinical cancer research : an official journal of the American Association for Cancer Research. 2009; 15:4058–4065. [PubMed: 19509148]

37. Wellbrock C, Hurlstone A. BRAF as therapeutic target in melanoma. Biochemical pharmacology. 2010; 80:561–567. [PubMed: 20350535]

38. Leslie EM, Deeley RG, Cole SP. Multidrug resistance proteins: role of P-glycoprotein, MRP1, MRP2, and BCRP (ABCG2) in tissue defense. Toxicology and applied pharmacology. 2005; 204:216–237. [PubMed: 15845415]

39. Zhou SF, Wang LL, Di YM, Xue CC, Duan W, et al. Substrates and inhibitors of human multidrug resistance associated proteins and the implications in drug development. Current medicinal chemistry. 2008; 15:1981–2039. [PubMed: 18691054]

Author Manuscript Author Manuscript Author Manuscript Author Manuscript

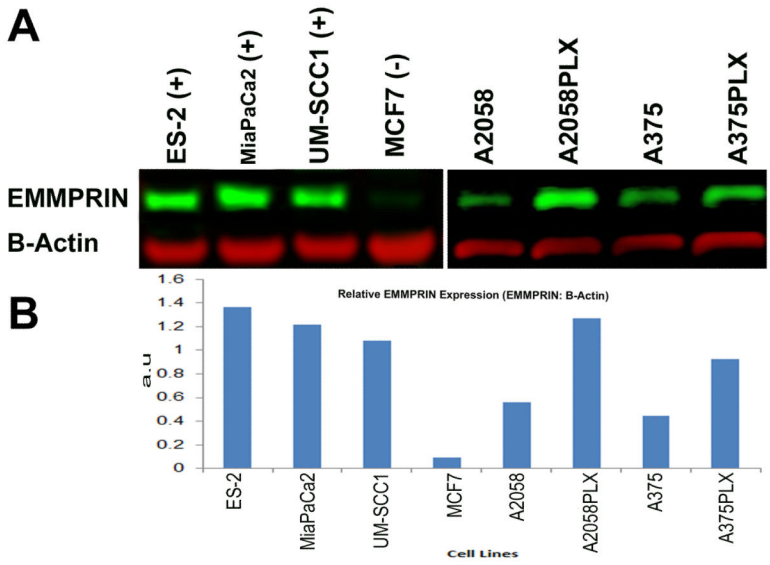

Figure 1.

Human melanoma cells lines express high levels of EMMPRIN. EMMPRIN is differentially expressed by Vemurafenib resistant cell lines A2058PLX and A375PLX. Control cell lines were ES-2 (clear cell ovarian cancer), MiaPaCa2 (pancreatic adenocarcinoma), UM-SCC1 (head and neck squamous cell carcinoma, and MCF 7 (breast cancer). (A) Western blot demonstrates increased EMMPRIN expression in PLX resistant cell lines. (B) Relative abundance of EMMPRIN to B-Actin was determined by dosimetry.

Author Manuscript Author Manuscript Author Manuscript Author Manuscript

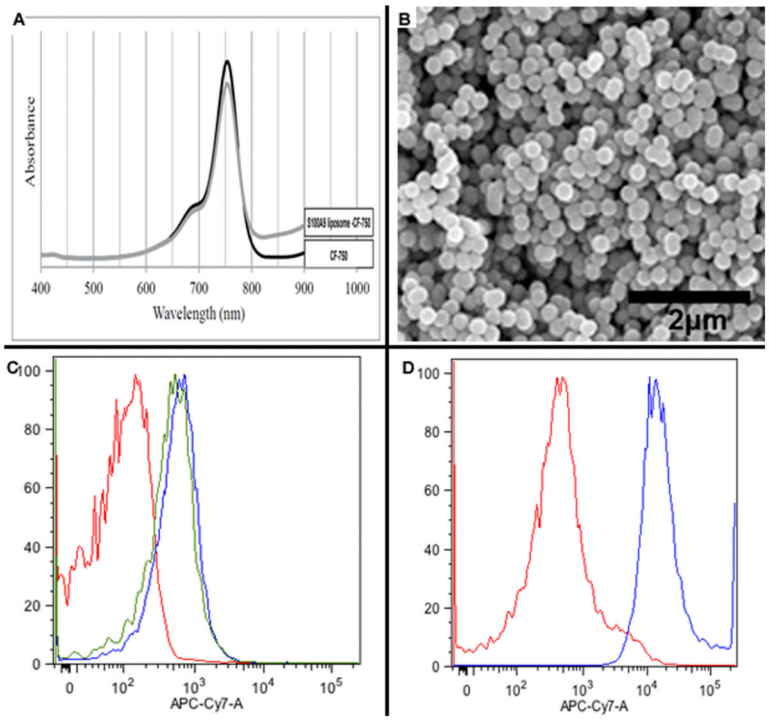

Figure 2.

Near-infrared (NIR) absorption spectra for CF-750 NIR dye demonstrates that absorption spectra is unchanged upon encapsulation within S100A9 liposome (A). SEM demonstrates that S100A9 liposomes are uniform in shape and are 200nm +/−30 nm diameter (B). Flow cytometry demonstrates that two separate batches of S100A9 probe bind to EMMPRIN expressing A2058 cells (C) and S100A9 liposome binds A2058 cells 100X more efficiently than untargeted liposome (D).

Author Manuscript Author Manuscript Author Manuscript Author Manuscript

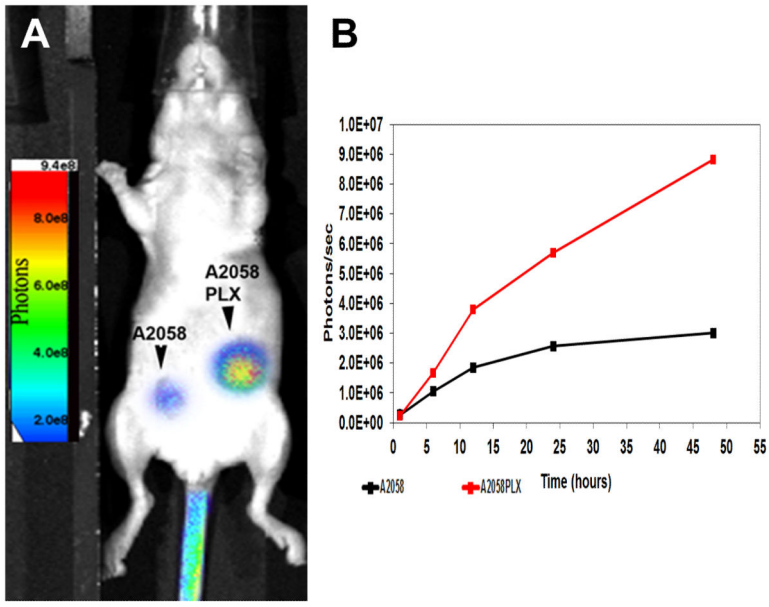

Figure 3.

In vivo Tumor accumulation of S100A9 probe occurs after 6 hr in separate subcutaneous melanoma tumors of A2058 and A2058PLX cells. (A) Mice injected iv with S100A9 liposomes at 5 O.D . AMIview images were taken every 6 h. (B) Regions of interest measurements were taken to determine accumulation of S100A9 liposomes. Significant increases were observed in A2058PLX resistant mice in comparison to A2058 p=0.001626.